Molecularly sensitive optical coherence tomography

Jeremy S. Bredfeldt,* Claudio Vinegoni,* Daniel L. Marks, and Stephen A. Boppart

Department of Electrical and Computer Engineering, Beckman Institute for Advanced Science and Technology, University of Illinois at Urbana-Champaign, 405 North Mathews Avenue, Urbana, Illinois 61801

Received August 10, 2004

Molecular contrast in optical coherence tomography (OCT) is demonstrated by use of coherent anti-Stokes Raman scattering (CARS) for molecular sensitivity. Femtosecond laser pulses are focused into a sample by use of a low-numerical-aperture lens to generate CARS photons, and the backreflected CARS signal is interferometrically measured. With the chemical selectivity provided by CARS and the advanced imaging capabilities of OCT, this technique may be useful for molecular contrast imaging in biological tissues. CARS can be generated and interferometrically measured over at least 600 μm of the depth of field of a low-numerical-aperture objective. © 2005 Optical Society of America

OCIS codes: 110.4500, 190.4410, 120.3180, 040.2840.

There are many clinical situations in which noninvasive, high-resolution imaging could be useful for locating and diagnosing pathological tissue. Optical coherence tomography (OCT) is being developed to fill this need.[1] In OCT, linear characteristics such as scattering, absorption, birefringence, and refractive index are measured to produce image contrast at near-histological resolutions. Unfortunately, these properties can be similar in different tissues, limiting the ability of OCT to distinguish between tissue types. To address this problem, two new OCT techniques are being studied that use molecular differences to provide more useful OCT contrast. The first technique uses exogenous contrast agents that can be targeted to bind to specific molecules to obtain molecular specificity.[2] The second technique, which was recently proposed[3] and demonstrated,[4] exploits coherent, nonlinear optical methods to identify endogenous molecular properties. Recently, second-harmonic OCT was used to image biological tissue.[5] Although second-harmonic OCT can differentiate between certain classes of tissue, unambiguous molecular identification cannot be achieved. Instead, we use a well-known optical molecular identification technique called coherent anti-Stokes Raman scattering (CARS).

In this Letter we present a first demonstration of a CARS-sensitive tomographic optical ranging technique for mapping the presence of a specific molecule within a sample. CARS is a vibrational spectroscopy technique that has found recent application in nonlinear microscopy.[6] The molecular selectivity of CARS has motivated its use as a molecular contrast mechanism for microscopy that alleviates the need for staining with fluorescent dyes to generate contrast as in confocal microscopy. In addition to its molecular identification capabilities, CARS is also emitted coherently with respect to the incident photons. Because of this coherent nature, CARS can be interferometrically measured. Our technique takes advantage of this property to provide molecular contrast for interferometric optical ranging in which the axial resolution is defined by the coherence length of the CARS pulse. One can improve axial resolution by increasing the bandwidth of the incident pulses at the expense of molecular specificity.

To achieve molecularly sensitive OCT, we use an interferometer similar to that used in traditional OCT. However, to generate CARS in the sample arm, we need a tunable Stokes pulse that is coherent with the pump. For the reference arm we need a coherent anti-Stokes pulse to obtain interference with the sample CARS pulse. A second-harmonic generation optical parametric amplifier (OPA) is used to produce the sample-arm Stokes and the reference-arm anti-Stokes pulses, both of which are coherent with each other since they are generated by the same pump.

We now describe in detail the experimental setup shown in Fig. 1. Ten percent of the output of a femtosecond, microjoule chirped-pulse amplification system (RegA 9000, Coherent, Inc.) is used as the pump pulse, whereas the rest is used to pump the second-harmonic generation OPA (OPA 9400, Coherent, Inc.). The output of the OPA consists of two pulses, the Stokes and the anti-Stokes, each separated in energy from the pump by an equal amount.

These input pulses represent the sources for our interferometer. We create the reference-arm pulse by separating the anti-Stokes pulse from the OPA output with a dichroic beam splitter, sending this reference pulse through a variable optical delay line, and coupling it into a 3-dB single-mode fiber coupler.

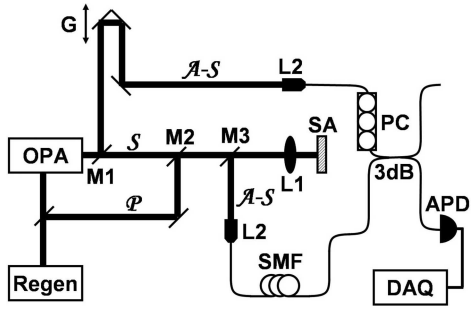

Fig. 1. Experimental setup: Regen, regenerative amplifier; G, galvanometer-controlled optical delay; M1–M3, long-pass dichroic mirrors with different cutoffs; $\mathcal{P}$, pump; $\mathcal{S}$, Stokes; $\mathcal{A}$-$\mathcal{S}$, anti-Stokes; L1, 30-mm focal-length lens; SA, sample; L2, 10× microscope objective; SMF, single-mode fiber; PC, polarization controller; APD, avalanche photodiode; DAQ, data acquisition.

0146-9592/05/050495-03$15.00/0

We then use an attenuated pump pulse from the amplifier and the Stokes pulse from the OPA, centered at 1047 nm, as the incident sample-arm pulses. These are collinearly and temporally overlap at another dichroic beam splitter and then are focused into the sample by use of an achromatic lens with a numerical aperture of 0.2. With a total incident power on the sample of 1.5 mW, anti-Stokes photons are generated at locations where the appropriate molecule is present. The backscattered photons are then separated out with a third dichroic beam splitter and coupled into the single-mode fiber coupler. As the reference-arm path length is scanned, the output of the fiber coupler is monitored with an avalanche photodiode operating in photon-counting mode. Finally, interference is measured and plotted as a function of delay position.

We first use acetone as the molecular species in our sample because it has a strong, isolated Raman-active vibrational mode at 2952 cm^{-1} associated with the C–H stretch vibration. The resulting CARS pulse is centered at 647 nm. The autocorrelation width, and thus the axial resolution, of this pulse is measured to be 32 μm (Fig. 2), and this signal is shown to result from a four-wave-mixing process since it is linearly related to the Stokes intensity and quadratically related to the pump intensity[4] (inset in Fig. 2). Moreover, this process is CARS resonance because, when the Stokes wavelength is tuned to the Raman-active vibrational mode in acetone, the anti-Stokes power is maximized.

The sample structure we use to demonstrate molecularly sensitive OCT is shown in Fig. 3(a). Two 100-μm-thick wells of acetone are sandwiched between 150-μm-thick coverslips. The thickness of each layer in the drawing represents the optical path length through the sample. An air-filled well, lined by two coverslips, is placed between the two wells of acetone physically separating them by approximately 600 μm. Forward-directed CARS photons are generated in each well of acetone and scattered from the glass slide interfaces. It is important to note here that this air gap is necessary to show that the signal measured from the second well of acetone is not simply backscattered CARS generated in the first well but, in fact, CARS generated from the second well. To prove that CARS is generated and backscattered from both wells of acetone, we place the sample such that the second layer of acetone is at the focus, and therefore the measured interference from this layer is greater in amplitude than that from the first.

Figures 3(b) and 3(c) show the demodulated interferometric axial measurement of the sample by use of standard OCT and molecularly sensitive OCT. Standard optical ranging [Fig. 3(b)] produces a reflection at each of the interfaces present in the sample, regardless of the presence of acetone. The molecular contrast ranging measurement [Fig. 3(c)] contains only two major peaks, which correspond to the two acetone layers in the sample. A strong, forward-directed CARS signal is generated in each acetone layer; therefore interference is measured only at the axial locations corresponding to the interfaces following these layers. The small peak at position 6 is likely the result of nonresonant four-wave mixing in the glass slide at that position. However, since the peak at position 7 has a much larger amplitude, we know that this peak is not simply due to the

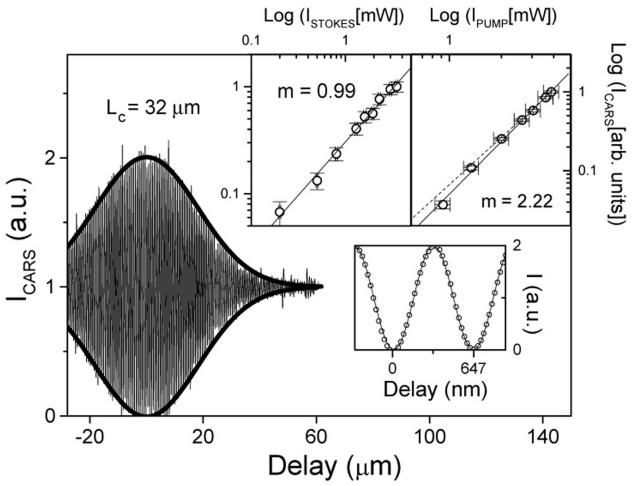

Fig. 2. CARS interferogram as measured from acetone. Inset, log–log plots of the intensity of the CARS signal.[4]

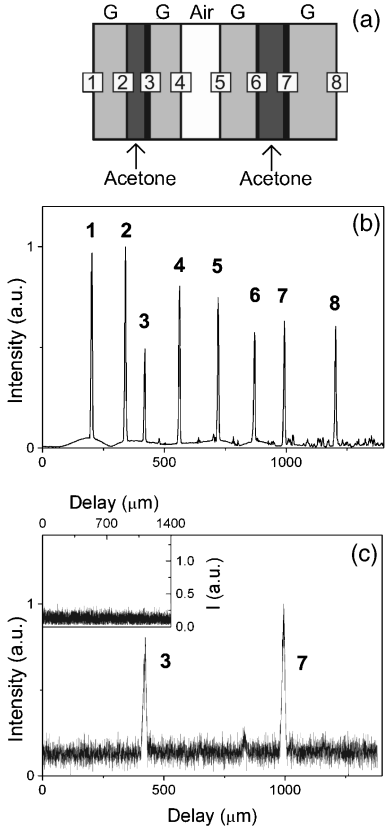

Fig. 3. (a) Schematic of the multilayer sample structure used to demonstrate molecularly sensitive interferometric ranging and OCT: G, glass. The thickness of each layer in the drawing represents the optical path length through that layer at the pump wavelength. Demodulated interferograms of the sample measured by (b) standard OCT and (c) CARS ranging. The inset in (c) shows demodulated interferometric data acquired in the absence of the Stokes pulses, indicating that CARS is generated only with the Stokes pulses present.

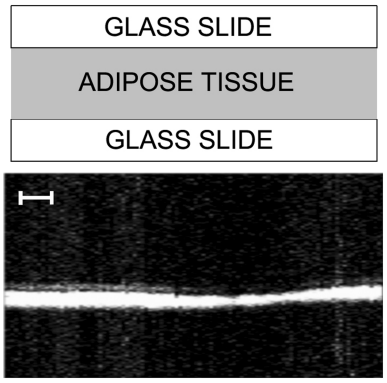

Fig. 4. Molecularly sensitive OCT image of the CARS signal generated from a thin, lipid-dense layer of beef tissue, sandwiched between two glass slides. The signal observed was mainly the result of forward CARS scattered off the tissue–glass interface. The scale bar represents 100 μm in both the axial and transverse directions.

subsequent backscatter of the forward-directed CARS from the first acetone layer. Since the interference results from scattering at the acetone–glass interface in each well, these peaks represent the point-spread function of the system. This result indicates that CARS can be generated and interferometrically measured over at least 600 μm of the depth of field of a low-numerical-aperture objective.

After demonstrating the axial ranging capabilities of this technique, a thin layer of lipid-dense beef tissue was compressed between two glass slides and placed in the sample arm to demonstrate biological imaging. The Stokes wavelength was tuned to excite a lipid resonance at 2845 cm^{-1}, and a dual-balanced photodetector was used. The two-dimensional image in Fig. 4 is the result of the CARS signal generated in the tissue sample and scattered from the tissue–glass interface. The nonuniform signal strength is the result of the varying thicknesses in the tissue layer. Each 500-μm axial scan required 10 s to acquire, which is limited by our delay line scanning apparatus. The acquisition time can be drastically improved with a spectral domain detection scheme. The measured signal-to-noise ratio (defined in a manner equivalent to OCT) is equal to 75 dB.

In conclusion, we have demonstrated molecularly sensitive optical ranging and OCT in a multilayer sample and biological specimen by combining the interferometric ranging technique used in OCT and the molecular identification capability of CARS. Although this research represents an important step toward molecularly specific OCT contrast, our setup has limitations in both sensitivity and specificity. The coupling efficiency of the backscattered CARS photons into the fiber currently limits our sensitivity and thus our ability to detect any weakly scattering interfaces within the lipid sample. In addition, the broad bandwidth of our current setup limits our molecular specificity. Pulse-shaping techniques[3] are therefore being developed to probe a wide range of biologically relevant resonances, such as the PO_2 phosphodiester resonances in nucleic acids, with high spectral resolution. In the future, this technique will improve OCT image contrast of biological tissues by differentiating between tissue types based on molecular composition rather than linear elastic scattering.

This research was supported in part by a research grant entitled A Nonlinear OCT System for Biomolecular Detection and Intervention from NASA and the National Cancer Institute (NAS2-02057, SAB). S. A. Boppart's e-mail address is boppart@uiuc.edu.

*These authors contributed equally to this work.

References

1. D. Huang, E. A. Swanson, C. P. Lin, J. S. Schuman, W. G. Stinson, W. Chang, M. R. Hee, T. Flotte, K. Gregory, C. A. Puliafito, and J. G. Fujimoto, Science **254,** 1178 (1991).
2. C. Yang, M. A. Choma, L. E. Lamb, J. D. Simon, and J. A. Izatt, Opt. Lett. **29,** 1396 (2004).
3. D. L. Marks and S. A. Boppart, Phys. Rev. Lett. **92,** 123905 (2004).
4. C. Vinegoni, J. S. Bredfeldt, D. L. Marks, and S. A. Boppart, Opt. Express **12,** 331 (2004), http://www.opticsexpress.org.
5. Y. Jiang, I. Tomov, Y. Wang, and Z. Chen, Opt. Lett. **29,** 1090 (2004).
6. J.-X. Cheng and X. S. Xie, J. Phys. Chem. B **108,** 827 (2004).